Journal of Materials Chemistry A

Accepted Manuscript

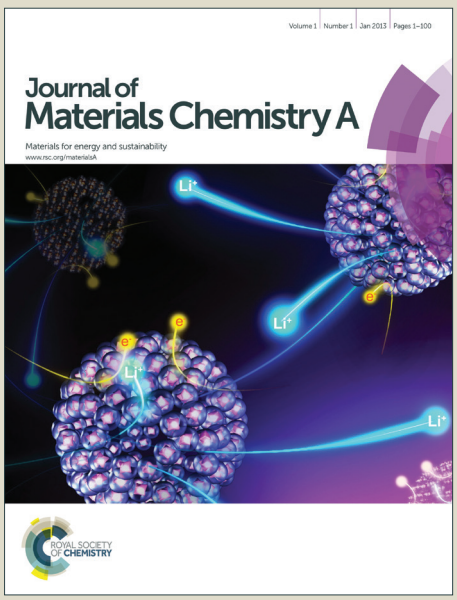

ROYAL SOCIETY OF CHEMISTRY

www.rsc.org/materialsA

Convenient and solventless preparation of neat carbon nanotube/polybenzoxazine nanocomposites with low percolation threshold and improved thermal and fire properties

Camilo Zúñiga[a], Leïla Bonnaud[b], Gerard Lligadas[a], Juan Carlos Ronda[a], Marina Galià[a], Virginia Cádiz[a] and Philippe Dubois*[b]

[a]Departament de Química Analítica i Química Orgànica. Universitat Rovira i Virgili. Campus Sescelades. Marcel.lí Domingo s/n. 43007 Tarragona. Spain.
Phone: (+34) 977 55 80 45. Fax: (+34) 977 558446
[b] Laboratory of Polymeric and Composite Materials, Center of Innovation and Research in Materials and Polymers (CIRMAP), Materia Nova Research Center & University of Mons, 23 Place du Parc, B-7000, Mons, Belgium. Fax: +32 (0)65 373484; Tel: +32 (0)65 373480;
E-mail corresponding author*: philippe.dubois@umons.ac.be

Keywords: Benzoxazine, carbon nanotubes, diphenolic acid, nanocomposite, percolation threshold, electrical properties, fire resistance, renewable resources.

Abstract

This work contemplates the use of pristine multi walled carbon nanotubes (MWNTs) as nanofillers in the bisphenol A-based polybenzoxazine and a diphenolic acid derived polybenzoxazine. The materials were prepared by a solventless method varying the MWNTs amount from 0.1 to 1.0 wt%. MWNTs were found to disperse well within both benzoxazine monomers and the dispersion also appears to be good in the cured system. Rheological and electrical percolation thresholds were obtained for MWNTs concentrations lower than 0.1 wt% indicating the existence of good affinity between MWNTs and polybenzoxazine matrices. The characterization of the resulting nanocomposites revealed that MWNTs affected differently the polybenzoxazines. The limiting oxygen index of the nanocomposites increased as a function of the nanotube content, from 35.2 to 38.7 for Bisphenol A- benzoxazine based system (BPA-PBz) and from 31.2 to 37.4 for Methyl 4,4'-bis-[6-(3-phenyl-3,4-dihydro-2H-1,3-benzoxazine)] pentanoate based system (MDP-PBz), respectively. Moreover, MWNTs positively influenced the thermo-mechanical, thermal and mechanical properties of the nanocomposites. The resulting attractive properties have been attributed to the good interactions between the polybenzoxazines and the finely dispersed nanofillers.

1. Introduction

Carbon nanotubes (CNTs) are considered of high interest for polymeric matrices not only for their excellent mechanical, thermal and electrical properties but also for their low density and high aspect ratio.[1] However, to exploit their maximum potential as reinforcing agents it is necessary to clear up some issues related to their poor dispersion, due to their tendency to form agglomerates, and a possible lack of interfacial adhesion between them and polymeric matrices. To solve these obstacles, chemical functionalization of CNTs has often been considered[2, 3, 4]. On occasions, this modification entails some constraints such as the deterioration of the CNTs walls and therefore the foreseen properties are affected [4, 5]. In addition, a drawback for its application in the industry is that their synthesis may require several steps. One valuable tool to assess the dispersion quality of nanoparticle-filled polymers is rheology[6]. By measuring the rheological parameters such as storage modulus, loss modulus and complex viscosity, it is possible to correlate with the filler dispersion, the inter-particle interaction and the polymer-filler interaction[6].

CNTs have been used to improve the electrical properties of non-conducting polymers as an alternative to common fillers such as carbon blacks and carbon fibers[7, 8]. According to the range of electrical conductivity exhibited by these nanocomposites, some applications include their use as electromagnetic interference (EMI)-shielding packages and wafer carriers for the microelectronics industry, electrostatic-assisted painting, fuel lines and filters that dissipate electrostatic charge in the automotive industry[9].

Among the many polymeric materials, polybenzoxazines have attracted significant attention of both industry and research community because of their unique advantages[10] becoming one of a rare few new polymers commercialized in the past 30 years. Polybenzoxazines can overcome the drawbacks of conventional phenolic resin synthesis by eliminating the release of byproducts during the curing reactions, the need of strong acid as catalyst and for toxic raw materials while retaining good thermal properties and flame retardancy of phenolic resins[11].

Polybenzoxazines with high flame retardant properties have gained attention owing to the increased demand for electronic materials[12]. Previous works on enhancement of the flammability properties of polybenzoxazines have been focused on the use mainly of phosphorus-[13-15], silicon-[16], and nitrogen-based[17] flame retardants. Most of them have been incorporated directly by chemical grafting onto the monomer through chemical modification of the amine or phenol precursors involved in the polybenzoxazine synthesis. Few studies have explored the dispersion of flame retardant additives on polybenzoxazines[18-20] and to our knowledge only very few researches have focused on the use of carbon-based nanostructures to infer flame retardancy[21].

The synthesis of bisphenol A-based benzoxazine (BPA-Bz) has been reported, and its polymerization yields thermosets with high structural integrity and thus the materials possess good properties. Unfortunately, bisphenol A (BPA) has shown to contribute significantly to an array of diseases and other health problems[22]. As a possible competitive alternative for BPA-Bz, it was proposed the synthesis of MDP-Bz (methyl 4,4´-bis-[6-(3-phenyl-3,4-dihydro-2H-1,3-benzoxazine)]pentanoate). This benzoxazine monomer is produced from the methyl ester (MDP) of renewable diphenolic acid (DPA)[23]. DPA is emerging as a potential "green" candidate to displace BPA because of its similar chemical structure, its lower price and because it has an extra functionality that can be involved for the polymer synthesis. In comparison with BPA-Bz, MDP-Bz has a higher glass transition temperature, a higher degradation temperature at 10% weight loss and superior thermo-mechanical properties[23].

Studies on the preparation and characterization of carbon-based/polybenzoxazine nanocomposites have been carried out using several benzoxazine monomers[24-28] and epoxy copolymers,[29-31] all of them, derived from non-renewable resources. As carbon-based nanofillers, pristine[28, 32], functionalized[26-28, 30, 31, 33] and surfactant treated multi walled carbon nanotubes (MWNTs)[29] as well as graphene[24, 25] have been used. The majority of these nanocomposites have been prepared using a solvent-based method, except when epoxy-benzoxazine mixtures were used[29, 31] and the carbon nanotubes were chemically grafted to the monomer[30]. CNT/polybenzoxazine nanocomposites are expected to find potential applications like molding compounds, adhesives in microelectronics[29], metal-like electrically conductive materials[24], superhydrophobic coatings[32] where improvements in thermal stability, hydrophobicity and electrical conductivity are required and expected.

In this study, the use of pristine MWNTs as nanofillers in BPA-Bz and MDP-Bz is explored. Nanocomposites were prepared by a convenient solventless method varying the MWNTs amount from 0.1 to 1.0 wt%. Moreover, the dispersion of the MWNTs within both benzoxazines was evaluated using rheological measurements and transmission electron microscopy. Finally, the characterization of the resulting materials was performed in terms of thermal, electrical, thermo-mechanical and fire properties.

2. Experimental Part

2.1. Materials

The following chemicals were obtained from Aldrich and used as received: ammonium sulphate, paraformaldehyde, 4,4´-bis(4-hydroxyphenyl) pentanoic acid, trimethyl orthoformate, p-toluenesulfonic acid monohydrate, toluene and methanol. 1,3,5-Triphenylhexahydro-1,3,5 triazine was synthesized as previously reported[23]. Bisphenol A-based benzoxazine (BPA-Bz) was supplied by Huntsman (Araldite MT 35600). Multiwalled carbon nanotubes (MWNTs) were provided by Nanocyl (NC7000) and were used without any further purification. According

to the supplier, the MWNTs have an average diameter of 9.5 nm, mean length of 1.5 μm, surface area ranging from 250 to 300 m^2/g and purity of ca. 90%.

2.2 Monomer Synthesis

Synthesis of methyl-4,4´-bis(4-hydroxyphenyl) pentanoate.

A 500 mL round bottom flask equipped with a condenser was charged with 4,4´-bis(4-hydroxyphenyl) pentanoic acid (0.26 mol), p-toluenesulfonic acid monohydrate ($2.6x10^{-4}$ mol), trimethyl orthoformate (0.38 mol) and 200 mL of methanol. The mixture was refluxed for 16 h, the methanol was removed under vacuum and the resulting syrup was dissolved in ethyl ether and washed several times with a $NaHCO_3$ saturated solution and with water. Finally, the ethyl ether was removed with a rotary evaporator and the product was dried under vacuum at room temperature. The resulting product was milled and used without further purification in the next step. A yield of 98% was obtained.

^{1}H NMR ($CDCl_3$/TMS, δ ppm): 7,05 (4H, d, J_o= 6.8 Hz), 6.73 (4H, d, J_o= 6.8), 4.68 (2H, s, OH) 3.62 (3H, s, OCH_3), 2.39 (2H, t), 2.10 (2H, t), 1.56 (3H, s).

^{13}C NMR ($CDCl_3$, δ ppm): 172.8 (s), 153.9 (s), 138.3 (s), 126.8 (d), 113.6 (d), 50.2 (q), 42.9 (s), 35.4 (t), 28.8 (t), 26.4 (q).

IR (ν cm^{-1}): 1700 (C=O st)

Synthesis of methyl 4,4´-bis-[6-(3-phenyl-3,4-dihydro-2*H*-1,3-benzoxazine)] pentanoate (MDP-Bz)

A 1 L two-necked round bottom flask equipped with a magnetic stirrer and a condenser was charged with 1,3,5-triphenylhexahydro-1,3,5-triazine (0.08 mol), paraformaldehyde (0.24 mol), methyl 4,4´-bis(4-hydroxyphenyl)pentanoate (methyl diphenolate) (0.12 mol) and 480 mL of toluene. The mixture was refluxed at 110°C for 20 h. After cooling to room temperature the benzoxazine monomer was filtered, dissolved in ethyl ether and washed 5 times with a 3N NaOH aqueous solution and with water. After washing, the organic phase was dried over sodium sulfate and the solvent was evaporated under vacuum at room temperature. A pale yellowish solid was obtained with a yield of 93%.

^{1}H NMR ($CDCl_3$/TMS, δ ppm): 7.32-6.74 (16H, Ar-H), 5.37 (4H, s, O-CH_2-N), 4.62 (4H, s, Ar-CH_2-N), 3.63 (3H, s, OCH_3), 2.40 (2H, t), 2.14 (2H, t), 1.56 (3H, s).

^{13}C NMR ($CDCl_3$, δ ppm): 174.4 (s, C=O), 152.5 (s), 148.5 (s), 141.2 (s), 129.3 (d), 126.9 (d), 125.3 (d), 121.3 (s), 120.3 (s), 118.0 (d), 116.6 (d), 79.2 (t, O-CH_2-N), 51.7 (q, OCH_3), 50.7 (t, Ar-CH_2-N), 44.6 (s), 36.6 (t), 30.1 (t), 27.8 (q).

IR (ν cm^{-1}): 1735 (C=O st)

2.3. Instrumentation

The FTIR spectra were recorded using a JASCO 680 FTIR spectrophotometer with a resolution of 4 cm^{-1} in the transmittance mode. An attenuated total reflection (ATR) accessory with thermal control and a diamond crystal (Golden Gate heated single-reflection diamond ATR, Specac, Teknokroma) was used.

^{1}H NMR 400Mhz and ^{13}C NMR 100.6 MHz NMR spectra were recorded using a Varian Gemini 400 spectrometer with Fourier Transform, $CDCl_3$ as solvent and TMS as internal standard.

Rheological measurements were performed on an ARES rheometer LS2 using a geometry of parallel plates (40 mm diameter) at a fixed gap of 0.5 mm. Frequency sweeps were carried out between 0.05 and 1000 rad/s at 120 ºC. The selected strain amplitude of 1% was checked to be in the linear viscoelastic range. The measurements were done on one representative sample.

Calorimetric studies were carried out at scanning rate of 20 ºC/min using a Mettler DSC821e thermal analyzer using N_2 as a purge gas (100 ml/min). Samples of about 5 mg were tested in closed aluminum pans by triplicate analysis. The calorimeter was calibrated with an indium standard (heat flow calibration) and an indium-lead-zinc standard (temperature calibration). Thermal stability study evaluated at a heating rate of 20 ºC/min using a TGA Q50 (TA instruments) with N_2 or air as a purge gas (60 mL/min) from 40 to 800 ºC. The reported thermograms were obtained with one representative sample.

Mechanical properties were measured using a dynamic mechanical thermal analysis (DMTA) apparatus DMA Q800. Specimens (10 mm x 54 mm x 2.6 mm) were tested in a three point bending configuration. The thermal transitions were studied in the 30-330ºC range at a heating rate of 3 ºC/min and at a fixed frequency of 1 Hz. One representative sample was used for the measurements.

Limiting Oxygen Index (LOI) measurements were performed using a Stanton Redcroft FTA flammability unit provided with an Oxygen Analyzer. A minimum of 4 samples (70 mm x 6 mm x 3 mm) were tested to evaluate LOI values. Samples were prepared by compression molding using an AGILA PE20 hydraulic press.

TEM images were obtained with a Philips CM200 instrument using an accelerating voltage of 120 kV. Samples of about 80 nm thick were prepared with a microtome (Leica

Ultracut UCT) at room temperature. The micrographs reported are representative morphologies observed at least at 3 different places.

Electrical measurements were performed on a Keithley multimeter 2700 measuring the resistance of the materials. Three different samples (6.0 mm x 12.2 mm x 2.7 mm) were previously coated with a silver paint for decreasing the contact resistance and then tested at room temperature.

2.4. Preparation of polybenzoxazine/MWNT nanocomposites

The nanocomposites were prepared by a solventless method using two different benzoxazine monomers: the commercial BPA-Bz and the synthesized MDP-Bz. A general method of preparation consisted of mixing an appropriate amount of MWNTs with benzoxazine followed by a melting at 120 ºC using a silicon oil bath. The mixture was then manually stirred and subsequently dispersed using an ultrasonic probe (Branson S-50D equipment, 200 W, 20 kHz, 13 mm diameter) for 1 min. After, the mixture was degassed in a vacuum oven at 140 ºC for 10 min and transferred to a stainless steel mold (cavity dimensions: 13 x 3 x 70 mm) for curing. The used amounts of MWNTs were 0.1, 0.3, 0.5 and 1.0 wt% of the total mixture weight. Polymerization of the mixtures was carried out using an AGILA PE20 hydraulic press at 135 bar according to the following curing conditions: 200 ºC for 2 h, 220 ºC for 2 h, 235 ºC for 3 h and 250 ºC for 3 h. A post-curing step was done at 250 ºC for 2 h in a conventional oven. A neat polybenzoxazine (without any MWNTs) was also prepared for the sake of comparison.

3. Results and discussion

3.1. Polybenzoxazine/MWNT nanocomposites

Thermosets from pristine MDP-Bz and BPA-Bz and their mixtures with different amounts of MWNT were carried out by thermal heating. Benzoxazine monomers undergo thermal ring opening to produce crosslinked polymers through Mannich bridges[34]. In the case of MDP-Bz, at high temperatures, additional crosslinks occur by transesterification between the ester groups and the phenolic OHs, formed during the ring opening of oxazines. (Scheme 1)[23].

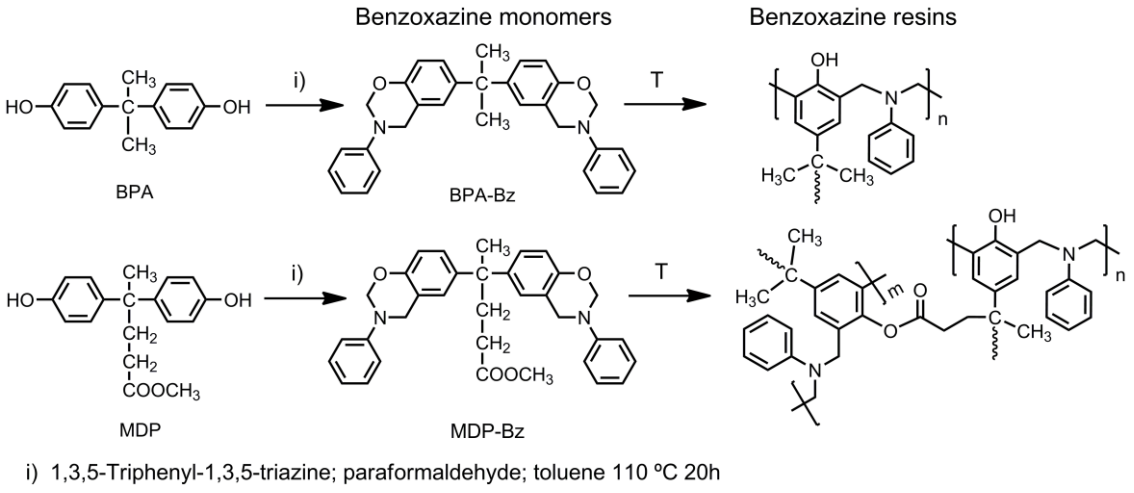

Scheme 1. Chemical structures of MDP-Bz and, BPA-Bz monomers and polybenzoxazines

3.2. Rheological properties

The main factors known to affect the performances of polymer/MWNT nanocomposites are the degree of dispersion of the MWNTs within the polymer matrix and the extent of interfacial adhesion between the MWNTs and the matrix[35]. In order to examine the dispersion state of MWNTs within both benzoxazine resins (*i.e.*, BPA-Bz and MDP-Bz), a rheological approach was applied to the systems prior curing (see Figure 1) as such a technique is known to be efficient to characterize the confinement and the dispersion of particles within a polymer matrix[6]. The viscosity sweep frequency curves of both benzoxazine pre-polymers reveal that their flow behavior is significantly modified in the presence of MWNTs. Indeed, neat BPA-Bz and MDP-Bz pre-polymers exhibit a Newtonian behavior whereas when MWNTs are incorporated in the benzoxazine monomers, a shear thinning behavior is observed. Storage modulus G' corresponding to the elastic properties and loss modulus G'' corresponding to viscous properties of the systems were also studied *versus* frequency. It appears that both neat benzoxazine monomers, similarly to epoxy uncured resins, follow the typical linear viscoelastic behavior of liquid whereas in both benzoxazine pre-polymers/MWNT suspensions, G' and G'' are found to increase very significantly with MWNTs content and frequency. More specifically, at low frequency, a plateau is noticed and a solid-like behavior is observed as G' values are found to be higher than G'' values even at a very low amount of MWNTs (i.e., 0.1 wt%). It is well known that MWNTs can organize themselves and generate an interconnecting network similar to a gel within liquid or molten polymers. This structural network is responsible for the enhancement and the almost frequency independence of G' and G'' at low frequency range (plateau apparition). In addition, the increase of G' plateau value observed with increasing MWNTs loading can be explained by the improvement of the network connectivity mainly

brought by the MWNTs particle interactions. It is worth noting that the transition from liquid-like to solid-like behavior occurs at a very low concentration of MWNTs (<0.1 wt%) suggesting that MWNTs exhibit very good interactions with both benzoxazines and disperse well within them. It is to note that the exact nature of these interactions is the subject of ongoing research. As benzoxazine molecules possess aromatic rings in their structures, CH-PI and PI-PI interactions may be involved[36]. In addition, nitrogen containing compounds are also known to develop attractive interactions with carbon nanotubes[37]. Thus, the nitrogen of benzoxazine structure may also be an active participant to the interactions between carbon nanotubes and benzoxazine molecules.

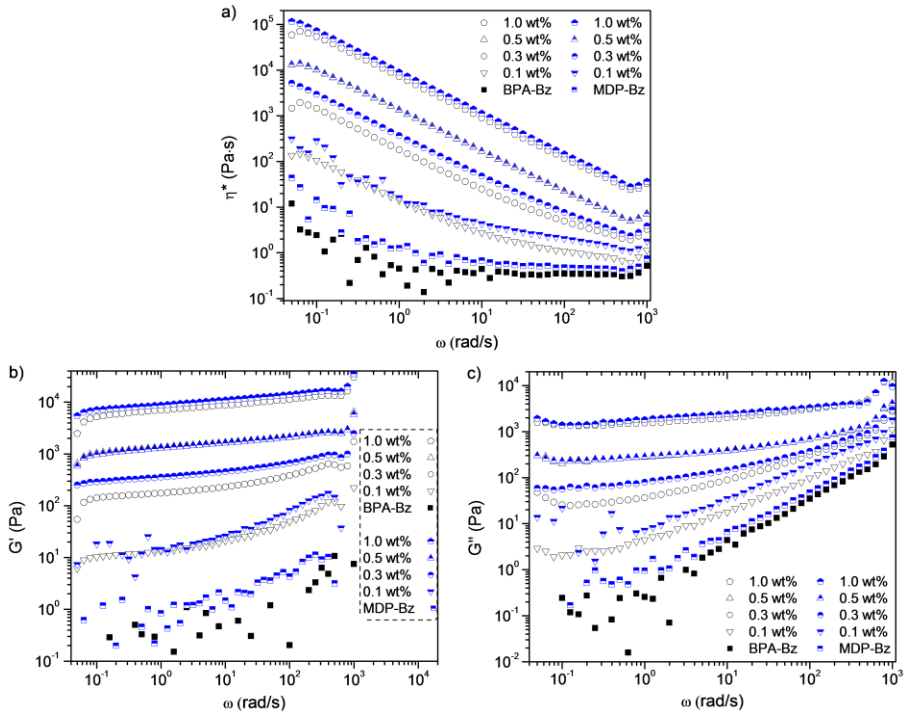

Figure 1. Frequency dependence of complex viscosity, storage modulus (G'), and loss modulus (G'') of BPA-Bz/MWNT and MDP-Bz/MWNT suspensions for different concentrations of MWNTs at 120°C.

3.3. Curing behavior of MWNT/Bz mixtures

It is reported in the literature that percolation threshold does not depend only on nanoparticle content but it is also very sensitive to the curing conditions of the nanocomposite.[38-41] In order to identify the possible action of MWNTs on benzoxazine polymerization, DSC testing was performed for both benzoxazines in the presence of different concentrations of MWNTs. Figure 2 represents the DSC thermograms of the unfilled monomers and MWNT/Bz mixtures at different MWNTs contents. It appears that in both monomer mixtures (MDP-Bz/MWNT and BPA-Bz/MWNT) there is a single exothermic peak (about 255°C for PBA-Bz based system and 265ºC for MDP-Bz based systems) associated with the

curing chemical processes, *i.e.*, the thermal ring-opening and crosslink reaction of benzoxazine functional groups. For both monomers (BPA-Bz and MDP-Bz), the addition of MWNTs causes a slight shifting of the maximum of the polymerization exotherms and the polymerization enthalpy of the mixtures progressively decreases with increasing content of MWCNT (from 178kJ/mol to 143kJ/mol for PBA-Bz based system and from 142kJ/mol down to 131kJ/mol for MDP-Bz based systems). This trend can be explained by the possibility for MWCNT to improve the thermal conductivity of the systems and better dissipate the polymerization heat.

For the sake of comparison, the curing conditions were kept the same for all the systems.

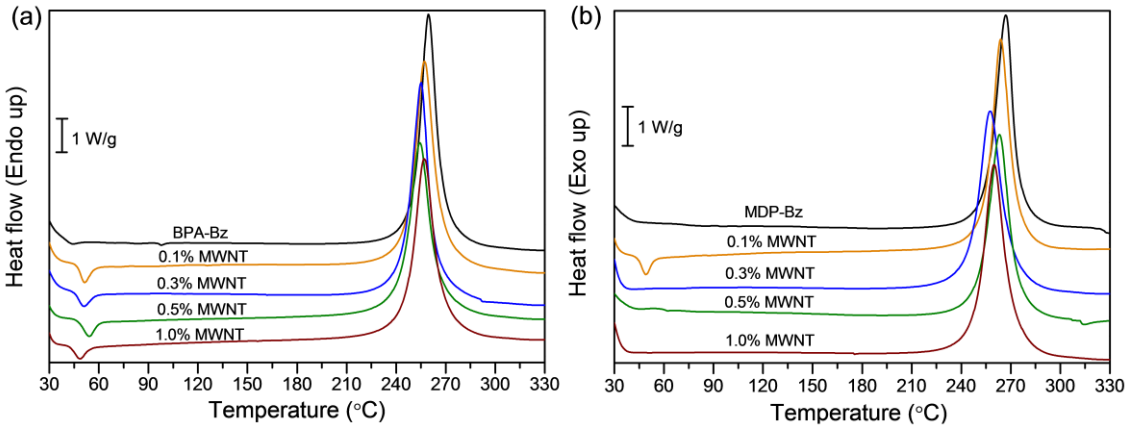

Figure 2. DSC thermograms of the unfilled monomers and a) MWNT/BPA-Bz and b) MWNT/MDP-Bz mixtures

Table 1: DSC data of the unfilled monomers, MWNT/BPA-Bz based systems and MWNT/MDP-Bz based systems

Sample	Enthalpy (kJ/mol)	T_{peak} (°C)
BPA-PBz	178	260
0.1 wt% MWNT	156	259
0.3 wt% MWNT	149	258
0.5 wt% MWNT	144	243
1.0 wt% MWNT	143	246
MDP-PBz	142	267
0.1 wt% MWNT	140	266
0.3 wt% MWNT	139	260
0.5 wt% MWNT	138	263
1.0 wt% MWNT	131	261

3.4. Morphology characterization of the nanocomposites

The distribution and the dispersion of pristine MWNTs within both polymer nanocomposites (MDP-PBz and BPA-PBz) after curing were examined by TEM. Representative images for 1.0 wt% MWNTs are shown in Figure 3. As can be seen, MWNTs are well distributed and dispersed within both polybenzoxazines highlighting there is no need for MWNTs surface functionalization to achieve their good dispersion within benzoxazine matrices. From TEM observations, it is not easy to differentiate MDP-PBz and BPA-Bz nanocomposite morphologies. However, CNT dispersion and distribution seem slightly better within MDP-PBz based system.

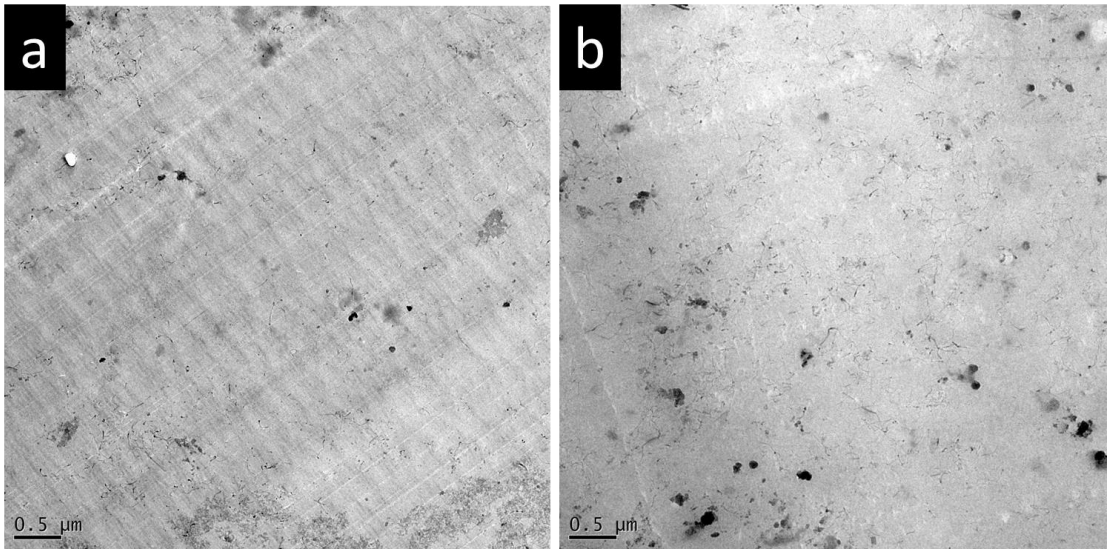

Figure 3. Representative TEM images of a) 1.0 wt% MWNT/BPA-PBz nanocomposites, b) 1.0 wt% MWNT/MDP-PBz nanocomposites

3.5. Electrical resistivity of the nanocomposites

The high aspect ratio of MWNTs, their fine dispersion and the formation of a "network-like" structure within the polymer matrix are key-parameters to endow polymers with improved electro-conductive properties. It was shown earlier in this paper that rheological percolation which requires contact between particles takes place at a very low concentration of MWNTs (< or = 0.1 wt%) for both BPA-Bz and MDP-Bz matrices. In addition, TEM analyses further highlighted the good dispersion of MWNTs within the matrices. Electrical measurements of MWNT-filled polybenzoxazine matrices gathered in Figure 4 are in good agreement with these results. Indeed, significant enhancement of electrical conductivity is obtained at a content in MWNTs as low as 0.1 wt%. Any further addition of MWNTs only increases slightly the electrical conductivity confirming the existence of a percolation threshold at a smaller concentration of MWNTs lower than 0.1 wt%.

In the literature, to the best of our knowledge, we only found one study that reports an electrical conductivity of 6.8 x10^{-5} S/cm (1.5 x 10^{4} Ω.cm) using 2.5 wt% of functionalized MWNT with benzoxazine groups[26]. In our case, better values were found at lower concentrations using pristine CNTs dispersed without the addition of a solvent. In fact, it is well known that functionalization often leads to damage partially the surface of CNTs and thus decrease their electrical properties[5]. MDP-Bz based nanocomposites are also found to exhibit slightly better electrical conductivity compared to BPA-Bz nanocomposites. Based on our experimental data, a possible explanation can lay on the difference of morphologies observed for MDP-Bz and BPA-Bz nanocomposites. Another assumption can be proposed to explain this result: it could also be related to the higher crosslinking degree of MDP-Bz which could lead to a higher and favourable immobilization of the MWCNT into the polymer matrix to facilitate the electron transport.

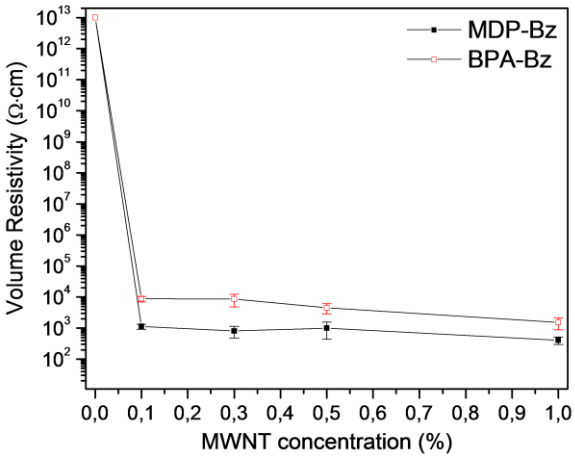

Figure 4. Electrical volume resistivity of BPA-PBz and MDP-PBz nanocomposites

3.6. Thermo-mechanical properties of the nanocomposites

The effect of MWNTs content on the glass transition temperature (Tg) of polybenzoxazine nanocomposites was determined using DMTA (as the maximum peak of tan δ) and DSC (as the half-height of the change in specific heat capacity, ½ Δ Cp). The Tg values from both measurements are shown in Table 2. Two different behaviors were observed according to the type of polybenzoxazine matrix (Fig. 5). Tg values for MDP-PBz nanocomposites, as expected, are found to be higher than BPA-PBz ones due to the transesterification reaction taking place between the ester group present onto each MDP-Bz monomer, and the hydroxyl group resulting from the opening of the oxazine ring[23].

For MWNT/BPA-PBz nanocomposites, Tg values of the materials do not seem to be significantly affected by the amount of MWNTs within the matrix. In addition, no marked

change is observed in the height of tan δ peak suggesting the MWNT content does not alter the crosslinking density of BPA-PBz.

For MWNT/MDP-PBz nanocomposites, the trend is different. More precisely, the presence of MWNTs triggers some important modifications of the Tg of the resulting materials. Quite interestingly, up to 0.5 wt% MWNTs, the recorded Tg values proved to increase, possible indication that interactions between the MWNTs and MDP-PBz are maintained after the crosslinking process, leading to a restriction of motion of the network in the nanocomposites. Moreover, the height of tan δ peak significantly decreased and becomes broader confirming the restriction of mobility of the crosslinked system in presence of MWNTs (<0.5 wt%)[26]. On the contrary, above 0.5 wt% MWNTs, Tg is observed to decrease to values lower than the Tg of neat MDP-PBz matrix. This phenomenon can be attributed to the volume saturation of the resin generating steric hindrance and preventing ester functional groups of the MDP-Bz matrix from reacting *via* transesterification leading to a decrease of the crosslinking density. In addition, it is to note that for MWNTs concentration higher than 0.5 wt%, the height of tan δ peak of MWNT/MDP-PBz systems is found to logically increase confirming the lower crosslinking density within the network allowing an increase of the network segment mobility.

Table 2: Tg values of the nanocomposites from DSC and DMTA

Sample	Tg (°C) from DSC (½ ΔC_p)	Tg (ºC) from DMTA (tan δ)
BPA-PBz	151	166
0.1 wt% MWNT	151	173
0.3 wt% MWNT	147	169
0.5 wt% MWNT	149	163
1.0 wt% MWNT	147	165
MDP-PBz	229	266
0.1 wt% MWNT	284	290
0.3 wt% MWNT	282	290
0.5 wt% MWNT	228	249
1.0 wt% MWNT	223	241

In addition to the thermo-mechanical transition which can be associated to the Tg of the materials, DMTA also allows to determining the temperature dependence of the storage modulus (E') for a material under shear deformation. For MWNT/BPA-PBz nanocomposites, in its glassy state, E' is observed to increase with the MWNTs content. The same trend is obtained for E' in the rubbery state. These improvements of E' are again indicative of good interactions between MWNTs and BPA-PBz leading to some restriction of chain mobility.

As far as MWNT/MDP-Bz nanocomposites are concerned, the presence of MWNTs leads to more radical change of E' in the glassy and rubbery states with respect to the related MWNT/BPA-PBz nanocomposites. Indeed, the addition of 0.1 wt% and 0.3 wt% of nanotubes results in an increase of E' whereas 0.5 wt% and 1.0% decreases E'. During the initial dispersion process of MWNTs within MDP-Bz, for low concentration of MWNTs (<0.5 wt%) interactions are tying down the MWNTs and the MDP-Bz chains leading to an increase of the crosslinking density and an increase of E' whereas for concentration of MWNTs higher than 0.5 wt%, the volume occupied by MWNTs becomes not neglectable and generates some steric hindrance preventing in some extent, esterification reactions to take place and hence the total curing of the forming network, resulting in a decrease of E'.

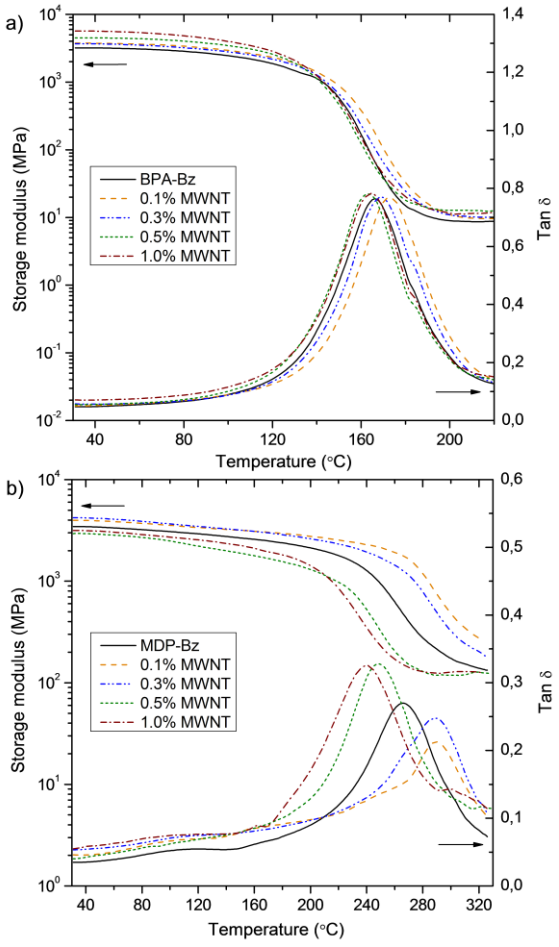

Figure 5. Effect of MWNTs content on storage modulus and tan δ plots of a) BPA-PBz nanocomposites and b) MDP-PBz nanocomposites

3.7. Thermal stability of the nanocomposites

To examine the effect of MWNTs on the thermal stability and the decomposition behavior of the polybenzoxazines, thermogravimetric analysis (TGA) was carried out under

nitrogen and air atmospheres. Figure 6 shows TGA and derivative thermogravimetric (DTG) curves and Table 3 summarizes TGA data for all the polymers. Polybenzoxazines based on diphenolic compounds, *e.g.*, BPA-PBz and MDP-PBz, usually present three stages of weight loss under (inert) nitrogen atmosphere. The first two weight loss stages are assigned to the volatilization of aniline (up to 300 ºC) and phenolic moieties (300-400 ºC), respectively, and the third one is related to the degradation of the char (above 400 ºC)[40]. Usually, the MDP-PBz exhibit higher thermal stability than the BPA-PBz as a consequence of a higher crosslinking density. It could be observed that the thermal properties of BPA-PBz and MDP-PBz were improved by incorporating MWNTs. Indeed, the addition of MWNTs induces a positive shift to higher temperatures in the decomposition temperatures of 1% ($T_{1\%}$) and 10% ($T_{10\%}$) weight loss. Similar results were reported in functionalized graphene/polybenzoxazine nanocomposites[25]. The main degradation temperature (T_{max}) of MWNT/MDP-PBz nanocomposites is slightly increased in comparison with the neat MDP-PBz. Moreover, it was observed that MWNTs promote the formation of char of the nanocomposites in comparison to neat polybenzoxazines, and more specifically the charring amount proved more important in the case of MWNT/MDP-PBz resins.

Table 3. Thermal properties and LOI values of polybenzoxazine nanocomposites

Sample	TGA (N_2)				TGA (Air)				LOI
	$T_{1\%}$ (°C)[a]	$T_{10\%}$ (°C)[b]	T_{max} (°C)[c]	Y_{800} (%)[d]	$T_{1\%}$ (°C)[a]	$T_{10\%}$ (°C)[b]	T_{max} (°C)[c]	Y_{800} (%)[d]	
BPA-PBz	241	388	438	33	254	409	416, 644	0.1	35.2
0.1 wt%	263	398	431	34	293	410	426, 658	0.1	36.4
0.3 wt%	283	399	433	35	297	407	424, 657	0.4	38.0
0.5 wt%	287	405	433	35	290	408	424, 667	0.2	38.5
1.0 wt%	281	401	433	35	289	410	427, 669	0.2	38.7
MDP-PBz	326	414	441	33	313	420	440, 608	0.2	31.2
0.1 wt%	359	414	448	33	373	417	445, 625	0.2	35.1
0.3 wt%	359	414	444	34	371	417	451, 623	0.3	36.4
0.5 wt%	334	420	448	36	344	424	444, 636	0.2	36.8
1.0 wt%	324	420	448	36	345	421	445, 638	0.2	37.4

[a] Temperature of 1% weight loss [b] Temperature of 10% weight loss
[c] Temperatures of maximum weight loss rate [d] Char yield at 800 °C

Under oxidative atmosphere, polybenzoxazines present two main processes related to the fragmentation of shift bases and the formation of char above 600 ºC. It was also observed a noticeable increase of ($T_{1\%}$) when 0.1 wt% and 0.3 wt% MWNTs were added to MDP-PBz, shifting from 313 ºC to 373 ºC and 371 ºC, respectively. The shift to higher temperatures in the first and most remarkable in the second peak of the degradation (T_{max}) of the polymers, attests

for the increase in thermal stability triggered by the addition of MWNTs. This delay was more evident for MDP-PBz at a concentration of 1.0 wt% MWNTs. However, it was not possible to observe any important influence in the char yield.

Usually, the above mentioned improvements in the thermal stability of the polymer nanocomposites are attributed to: 1) the good dispersion of MWNTs which might hinder the flux of degradation products from the polymer into the gas phase delaying the onset of degradation; 2) the strong interfacial interactions between the polybenzoxazines and MWNTs restrict the mobility of the polymer chains near the nanotubes causing a delay in their degradation and therefore shifting T_{max} to higher temperatures and 3) the higher thermal conductivity in the polymer/nanotube nanocomposites that could ease heat dissipation within the materials[41].

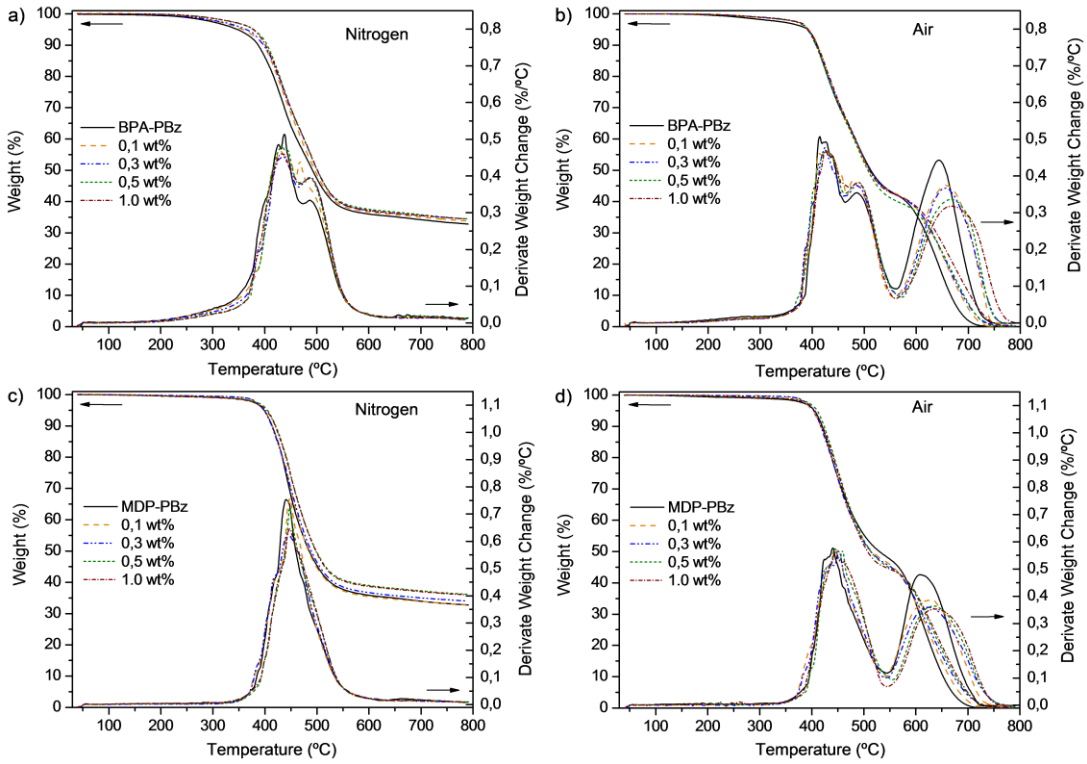

Figure 6. TGA and DTG plots of MWNT/BPA-PBz and MWNT/PBz-MDP nanocomposites in nitrogen (a and c) and air atmospheres (b and d), respectively.

3.8. Flame retardant properties of the nanocomposites

Limiting Oxygen Index (LOI) defined as the minimum fraction of oxygen in a gas mixture of oxygen and nitrogen that can bear flaming combustion is a useful indicator to evaluate the flammability of the materials. The LOI values of the polybenzoxazine-based systems are collected in Table 3. They are found to increase with the content of MWNTs. The

enhancement is slightly better in the case of MDP-PBz nanocomposites when compared to BPA-PBz counterparts and it is worth noting that low amounts of MWNTs (0.1 wt% and 0.3 wt%) already allow for achieving significant improvement of flame retardancy of both nanocomposites. It has been evidenced in the literature that the degree of dispersion affects the extent of the results and in presence of finely dispersed MWNTs, polymeric nanocomposites exhibit a greater flame retardancy behavior[42-43], which is in agreement with our results. Moreover, LOI values are found to follow a similar trend with the char yield obtained by TGA. The LOI values obtained for both polybenzoxazine systems stress the beneficial effect of MWNTs to impart flame retardancy. It has been demonstrated that carbon nanotubes can reduce the flammability of materials through the formation of a continuous protective layer consisting of a network of nanoparticles that serves as a heat shield and re-emits much of the incident radiation back decreasing the polymer degradation rate and hinders the attack of the matrix by oxygen radicals[44-45].

4. Conclusions

Polybenzoxazine nanocomposites containing MWNTs were successfully prepared following a convenient and solventless process. The addition of MWNTs to both monomers did not interfere with the ring opening of the benzoxazines. Rheological measurements showed that benzoxazine/MNWT mixtures presented a low percolation threshold (< or = 0.1 wt%) indicating a well dispersion state derived from the strong interactions between nanofillers and both monomers. TEM and electrical properties of the crosslinked polybenzoxazine nanocomposites confirmed the preservation of the good dispersion state after their curing. The electrical percolation threshold was in agreement with rheological results and it was found to take place at a concentration lower or equal to 0.1 wt% for both polybenzoxazine resins. The thermal stability of both nanocomposites was significantly affected by the amount of MWNTs, especially in the initial degradation step. The Tg of the MWNT/BPA-PBz nanocomposites was not affected by the MWNTs content whereas for MWNT/MDP-PBz counterparts, concentrations lower than 0.5 wt% significantly increased the Tg values. The good dispersion state of MWNTs and their good affinity with both resins induced a meaningful effect that was reflected in an increase of the storage modulus E' in both glassy and rubbery states and an enhancement in the char yield and fire behaviour (LOI) of the polybenzoxazine nanocomposites. It is worth noting that these promising results were obtained with pristine MWNTs and they did not require any surface treatment nor functionalization to promote their dispersion within the benzoxazine matrices.

Acknowledgments

The authors wish to thank the "Région Wallonne" for the financial support in the framework of ECOTAC project from the "Pôle de compétitivité SKYWIN" and the Interuniversity Attraction Poles Programme initiated by the Belgian Science Policy Office. MATERIA NOVA and CIRMAP thank the European Community for general support in the frame of the 7th Framework research project "IASS", the ''Belgian Federal Government Office Policy of Science (SSTC)'' for its support in the frame of the PAI-6/27 and the ''Région Wallonne'' in the framework of the ''Programme d'Excellence : OPTI²MAT and FLYCOAT''. We thank Yoann Paint for the help on TEM. Authors also thank Nanocyl S. A. (Belgium) for kindly providing MWNTs and Huntsman Advanced Materials (Europe) for kindly supplying the BPA-Bz resin. The authors also express their thanks to CICYT (Comisión Interministerial de Ciencia y Tecnología) (MAT2011-24823 Spain) for financial support.

References

1. M. Terrones, *Annu. Rev. Mater. Res.*, 2003, **33**, 419-501.
2. K. Balasubramanian and M. Burghard, *Small*, 2005, **1**, 180-192.
3. D. Tasis, N. Tagmatarchis, A. Bianco and M. Prato, *Chem. Rev.*, 2006, **106**, 1105-1136.
4. P.C. Ma, N.A. Siddiqui, G. Marom, J.K. Kim, *Composites Part A*, 2010, **41**, 1345-1367.
5. L. Liu, K.C. Etika, K.S. Liao, L.A. Hess, D.E. Bergbreiter, J.C. Grunlan, *Macromol. Rapid Commun.*, 2009, **30**, 627-632.
6. Q. Zhang, F. Fang, X. Zhao, Y. Li, M. Zhu and D. Chen, *J. Phys. Chem. B*, 2008, **112**, 12606-12611.
7. M. H. Al-Saleh, W. H. Saadeh and U. Sundararaj, *Carbon*, 2013, **60**, 146-156.
8. L. Bonnaud, O. Murariu, N. De Souza Basso and P. Dubois, *Polym. Bull.*, 2013, **70**, 895-904.
9. M. F. L. De Volder, S. H. Tawfick, R. H. Baughman and A. J. Hart, *Science*, 2013, **339**, 535-539.
10. H. Ishida, in *Handbook of Benzoxazine Resins*, eds. I. Hatsuo and A. Tarek, Elsevier, Amsterdam, 2011, pp. 3-81.
11. N. N. Ghosh, B. Kiskan and Y. Yagci, *Prog. Polym. Sci.*, 2007, **32**, 1344-1391.
12. V. Cádiz, J. C. Ronda, G. Lligadas and M. Galià, in *Handbook of Benzoxazine Resins*, eds. I. Hatsuo and A. Tarek, Elsevier, Amsterdam, 2011, pp. 556-576.
13. H. Ling and Y. Gu, *J. Macromol. Sci., Phys.*, 2011, **50**, 2393-2404.
14. M. Spontón, J. C. Ronda, M. Galià and V. Cádiz, *Polym. Degrad. Stab.*, 2008, **93**, 2158-2165.
15. L.-K. Lin, C.-S. Wu, W.-C. Su and Y.-L. Liu, *J. Polym. Sci., Part A: Polym. Chem.*, 2013, **51**, 3523-3530.
16. M. Spontón, D. Estenoz, G. Lligadas, J. C. Ronda, M. Galià and V. Cádiz, *J. Appl. Polym. Sci.*, 2012, **126**, 1369-1376.
17. D. Wang, B. Li, Y. Zhang and Z. Lu, *J. Appl. Polym. Sci.*, 2013, **127**, 516-522.
18. C. Zúñiga, G. Lligadas, J. C. Ronda, M. Galià and V. Cádiz, *Polymer*, 2012, **53**, 1617-1623.
19. S. Rimdusit, N. Thamprasom, N. Suppakarn, C. Jubsilp, T. Takeichi and S. Tiptipakorn, *J. Appl. Polym. Sci.*, 2013, **130**, 1074-1083.
20. C. H. Lin, S. X. Cai, T. S. Leu, T. Y. Hwang and H. H. Lee, *J. Polym. Sci., Part A: Polym. Chem.*, 2006, **44**, 3454-3468.
21. L. Dumas, L. Bonnaud, M. Olivier, M. Poorteman and Ph. Dubois, *Chem. Commun.*, 2013, **49**, 9543-9545

22. C. E. Talsness, A. J. M. Andrade, S. N. Kuriyama, J. A. Taylor and F. S. vom Saal, *Phil. Trans. R. Soc. B*, 2009, **364**, 2079-2096.
23. C. Zúñiga, M. S. Larrechi, G. Lligadas, J. C. Ronda, M. Galià and V. Cádiz, *J. Polym. Sci., Part A: Polym. Chem.*, 2011, **49**, 1219-1227.
24. M. Zeng, J. Wang, R. Li, J. Liu, W. Chen, Q. Xu and Y. Gu, *Polymer*, 2013, **54**, 3107-3116.
25. K.-K. Ho, M.-C. Hsiao, T.-Y. Chou, C.-C. M. Ma, X.-F. Xie, J.-C. Chiang, S.-h. Yang and L.-H. Chang, *Polym. Int.*, 2013, **62**, 966-973.
26. Y.-H. Wang, C.-M. Chang and Y.-L. Liu, *Polymer*, 2012, **53**, 106-112.
27. J.-M. Huang, M.-F. Tsai, S.-J. Yang and W.-M. Chiu, *J. Appl. Polym. Sci.*, 2011, **122**, 1898-1904.
28. Y. Liu, B. Wang and X. Jing, *Polym. Compos.*, 2011, **32**, 1352-1361.
29. M. Kaleemullah, S. U. Khan and J.-K. Kim, *Compos. Sci. Technol.*, 2012, **72**, 1968-1976.
30. M. Xu, J. Hu, X. Zou, M. Liu, S. Dong, Y. zou and X. Liu, *J. Appl. Polym. Sci.*, 2013, **129**, 2629-2637.
31. L. Yang, C. Zhang, S. Pilla and S. Gong, *Composites Part A*, 2008, **39**, 1653-1659.
32. C.-F. Wang, H.-Y. Chen, S.-W. Kuo, Y.-S. Lai and P.-F. Yang, *RSC Advances*, 2013, **3**, 9764-9769.
33. Q. Chen, R. Xu and D. Yu, *Polymer*, 2006, **47**, 7711-7719.
34. H. Hishida, D.P. Sanders, *Polymer*, 2001, **42**, 3115-3125
35. M. Chapartegui, N. Markaide, S. Florez, C. Elizetxea, M. Fernandez and A. Santamaría, *Compos. Sci. Technol.*, 2010, **70**, 879-884.
36 C. Oueiny, S. Berlioz, F.X.Perrin, *Prog. Polym. Sci.*, 2013, http://dx.doi.org/10.1016/j.progpolymsci.2013.08.009.
37 J.M. Brown, D.P. Anderson, R.S. Justice, K. Lafdi, M. Belfor, K.L. Strong, D.W. Schaeffer, *Polymer*, 2005, **46**, 10854-10865.
38. G. Faiella, V. Antonucci, S. T. Buschhorn, L. A. S. A. Prado, K. Schulte and M. Giordano, *Composites Part A*, 2012, **43**, 1441-1447.
39. G. Olowojoba, S. Sathyanarayana, B. Caglar, B. Kiss-Pataki, I. Mikonsaari, C. Hübner and P. Elsner, *Polymer*, 2013, **54**, 188-198.
40. H. Yee Low and H. Ishida, *Polymer*, 1999, **40**, 4365-4376.
41. M. Moniruzzaman and K. I. Winey, *Macromolecules*, 2006, **39**, 5194-5205.
42. T. Kashiwagi, F. Du, K. I. Winey, K. M. Groth, J. R. Shields, S. P. Bellayer, H. Kim and J. F. Douglas, *Polymer*, 2005, **46**, 471-481.
43. S. Bourbigot, S. Duquesne and C. Jama, *Macromol. Symp.*, 2006, **233**, 180-190.
44. T. Kashiwagi, E. Grulke, J. Hilding, K. Groth, R. Harris, K. Butler, J. Shields, S. Kharchenko and J. Douglas, *Polymer*, 2004, **45**, 4227-4239.
45. S. Bocchini, A. Frache, G. Camino and M. Claes, *Eur. Polym. J.*, 2007, **43**, 3222-3235.